QUANTITATIVE DESCRIPTION OF MC, M_2C, M_6C AND M_7C_3 CARBIDES IN HIGH SPEED STEEL ROLLS

L. DE COLNET[1] – E. PIRARD[1] – J. TCHOUFANG TCHUINDJANG[2] – J. LECOMTE-BECKERS[2] – R. GFHIRI[3]– P. BOERAEVE[3] – S. CESCOTTO[3]

University of Liège, [1]MICA laboratory, D2, Avenue des Tilleuls 45, 4000 Liège, Belgium; [2]Met. and Mat. Sc., [3]MSM Department, B52/3,Chemin des Chevreuils 1, 4000 Liège, Belgium.

ABSTRACT

One goal of the COST 517 project entitled "Effects of inclusions and carbides on the mechanical properties of alloyed steels" is to establish quantitative and statistical relations between the microstructure and the mechanical properties of rolls materials. This paper presents the different steps necessary to characterise the microstructure and the carbides presents in high-speed steel rolls. First, carbides were examined by SEM and EDX microscopy. Then, images of samples were acquired by optical microscopy and analysed to finally measure quantitative parameters describing the grains and the carbides.

KEY WORDS

High speed steel, carbides, grain size, image analysis.

INTRODUCTION

For the last years high speed steels (HSS) rolls have been introduced in the hot strip mills. Nowadays they are used in the front stand of a finishing section (mainly in Japan). HSS possesses excellent wear resistance due to the presence of hard carbides .and can therefore be used for longer rolling campaigns, increasing the hot strip mill productivity

The materials studied come from shell rolls (60 mm thick) made of high-speed steel (Figure 4). The raw material was elaborated in the industrial plant, according to common industrial practice. The casting process consists in a vertical spun casting, where the shell metal is first poured to form the subsequent barrel, then is followed by the casting of the core metal which is in SG iron .The shell, directly in contact with the rolled sheets, is submitted to high thermal and mechanical stresses. So, its microstructure is the important feature to be characterised. The average composition of the material is given in Table 1

Table 1. Average composition of HSS7 (% Weight).

Grade	%C	%Si	%Mn	%Ni	%Cr	%Mo	%W	%V
HSS7	*1.5/2.0*	*0.5/1.0*	*0.5/1.5*	*1.0/1.5*	*5/7*	*2/5*	*1/3*	*3/5*

EXPERIMENTAL

Qualitative Carbide description

In order to determine the nature of the different carbides encountered in the studied material, a Nital (3%) etching was made on a polished sample coming from the shell. The nature of the carbides is determined by means of electron microscopy (SEM and EDX), and the results are

given in Table 2. Four groups of carbides were found in HSS7: MC (rich in V), M_2C (rich in Mo), M_6C (rich in W and Mo) and M_7C_3 (rich in Cr). Figure 1 shows an overview of carbides (SEM) and Figure 2 illustrates the associated mapping, obtained while using EDX.

Table 2. General characterization of carbides in HSS7

Types of carbides	***Composition*** *(EDX mapping)*	***Shape*** *(Distribution)*	***Contrast with secondary e⁻*** *(SEM)*	***Colour towards GROESBECK's reagent*** *(OM)*
MC	V (most present element) Mo, W, Cr	Bulky lobules or Aggregates "Coral-like"	Dark to dark gray	Light Pink
M_2C	Mo, W (most present elements) V, Cr	Acicular (Herringbone-like) Or Lamellae	White to light gray	Dark brown
M_7C_3	Cr (most present element) V, Mo Fe (slight traces)	"Fishbone-like" or Lamellae	Gray	Yellow
M_6C	Mo, W (most present elements) V	"Fishbone-like" (with lamellas more tiny than those in **M_7C_3**)	White	Blue

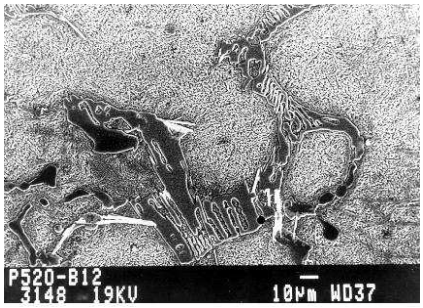

Fig. 1. Carbides on HSS7 (working surface of the roll: Surface 2 on Figure 4)

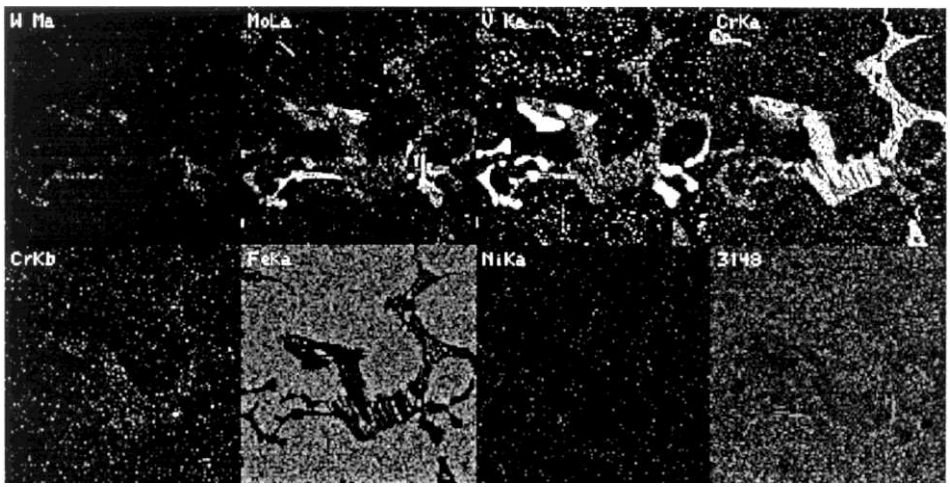

W (M_α) ***Mo (L_α)*** ***V (K_α)*** ***Cr (K_α)***

Cr (K_β) ***Fe (K_α)*** ***Ni (L_α)***

Fig. 2. Mapping associated to Figure 1 (6 elements selected: W, Mo, V, Cr, Fe et Ni)

Furthermore, Groesbeck's reagent [1] was used to differentiate each group of carbides, by means of optical microscopy. MC carbides are not etched and appear in pink in the matrix; M_2C in dark brown and M_7C_3-M_6C in blue or yellow. Both M_6C and M_7C_3, which are always associated and have the same colour, have to be considered as a whole when using optical microscopy (Figure 3).

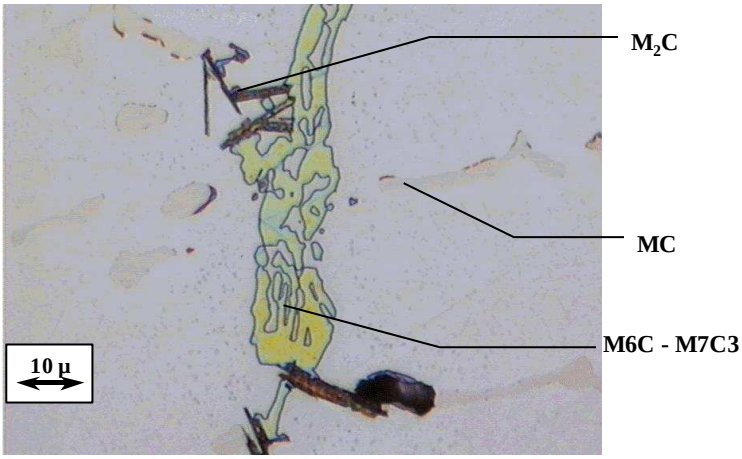

Fig. 3. Carbide image after Groesbeck's etching: M_6C - M_7C_3 (Yellow) - Acicular M_2C (Brown) - MC (light pink globules).

Sample Preparation

Preliminary observations of the shell under an optical microscope show microstructural differences from the surface to the shell-core limit (an increase in the grain and carbide size). Samples are obtained from a bar cut in the shell of the roll. In order to study carbide variations as a function of the distance to the surface, several samples are prepared to cover all the shell depth. Carbide variations are also studied in each of the three main directions of the roll: the surface 1 is obtained if the roll is cut longitudinally; surface 2 if it is cut perpendicular to the radius of the cylinder and surface 3 if it is cut transversally.

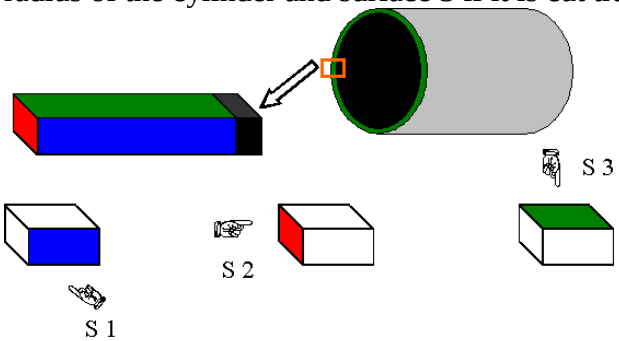

Fig. 4. Sample preparation.

Image acquisition

Digital images from the etched samples (Groesbeck's etching) were acquired under an optical microscope using a 12 bit Peltier cooled CCD camera with a maximum resolution of 1280 by 1024 squared-pixels. Two magnifications were used during the study (Table 3).

An interferential filter with a very narrow bandwidth (10 nm at half maximum transmission peak) is put in front of the camera to improve contrast between carbides and matrix. On Figure 6, contrast between the MC and the matrix is improved. Peaks of these two phases are well separated with a filter and confused without.

Table 3. Image calibrations

Distance between two pixels (a_0).	Width of the field (1280 columns)	Height of the field (1024 lines)
0.44 µm	563.2 µm	450.6 µm
0.88 µm	1126.4 µm	901.2 µm

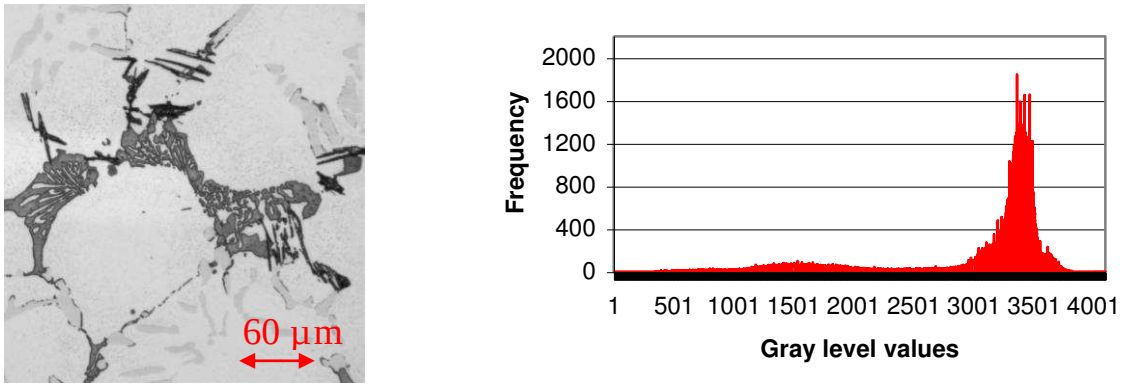

Fig. 5. Image acquired for the whole spectral range (white light) and its grey level histogram.

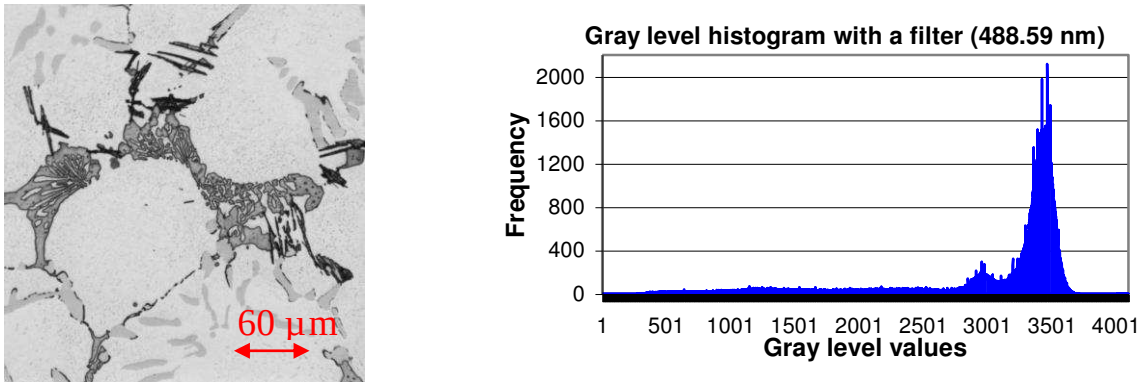

Fig. 6. Image acquired at 488 nm (±10 nm) and its grey level histogram.

Image processing

First, carbides and matrix are separated by a simple thresholding. Because the etching is not totally reproducible from one sample to another and sometimes heterogeneous on the sample surfaces, the operator for every image chooses threshold levels interactively. Secondly, isolated MC carbides are easily extracted thanks to their average grey level (Figure 6). After these two first operations, unclassified pixels are MC, M_2C and M_7C_3-M_6C carbides belonging to clusters.

Pixels are finally assigned to one of the three carbide types (MC, M_2C or M_7C_3-M_6C) on the basis of their grey level value and of some criteria. For example, around and inside M_2C-M_7C_3-M_6C carbides, matrix is digitised by pixels with grey level values equal to those of the MC because they are a transition between a bright matrix and darker carbides. So, one criterion is to assign these pixels to the matrix. Three binary images of every kind of carbides are finally obtained. Any combination of these images can be considered, like image of all carbides.

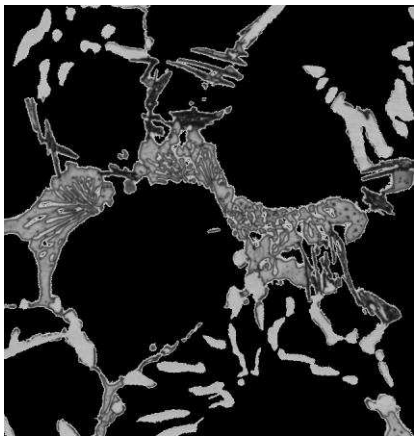

Fig. 7: Result of the simple thresholding with in black pixel of the matrix.

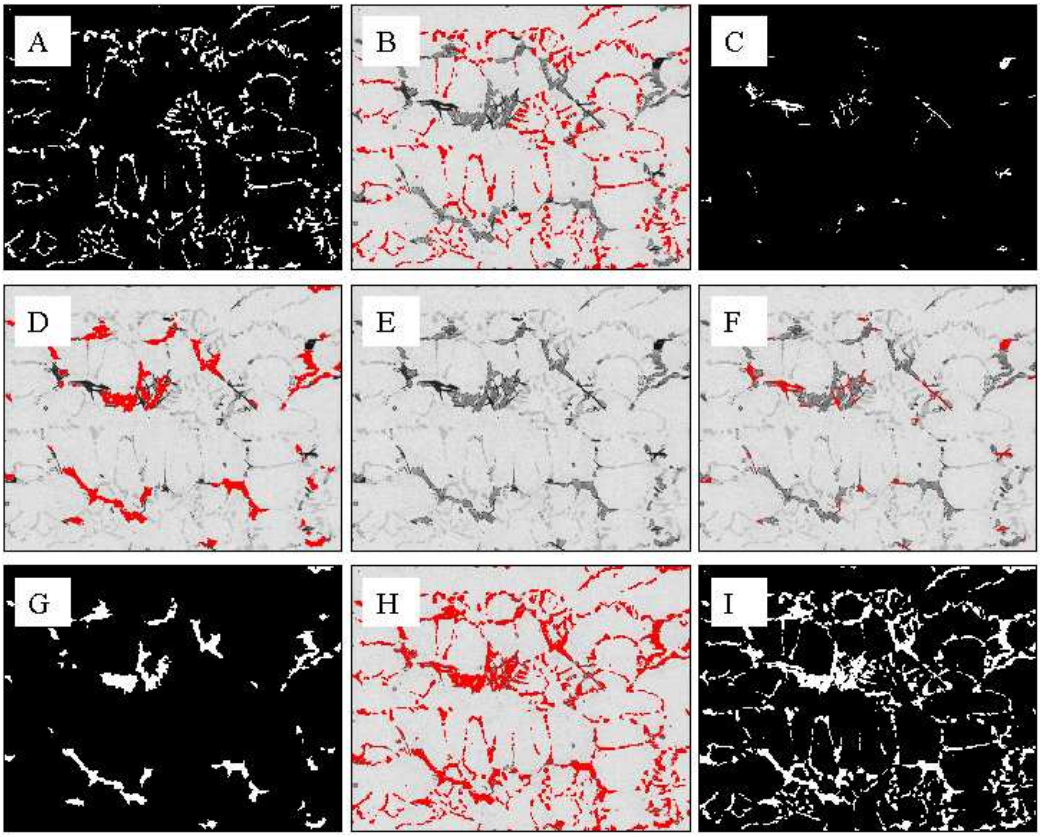

Fig. 8: Carbide segmentation. A: MC binary image. B: MC carbides. C: M_2C binary image. D: M_7C_3-M_6C carbides. E: Initial image. F: M_2C carbides. G: M_7C_3-M_6C binary image. H: Carbides. I: Carbide binary image.

Measurements

Many parameters are measurable on binary images to describe grains or carbides (volume fraction, size, shape, spatial distribution…). Among all these parameters, the carbide area fraction is measured without carbide differentiation or type by type. From the first stereological principle [2], the area fraction is an unbiased estimator of the volume fraction.

The size of the MC and M2C carbides is described by the length of the major and minor axes of the ellipse with equivalent moments of inertia [3].

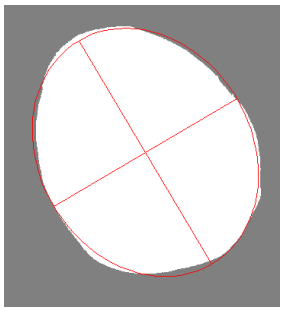

Fig. 9: Ellipse of inertia.

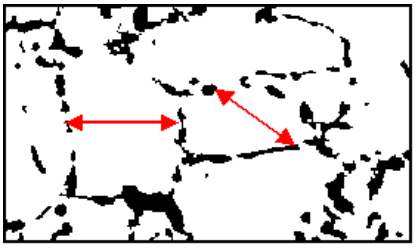

Fig. 10: Example of intercept length measured inside the grain phase.

A measure of the skeleton length of the M_6C-M_7C_3 and carbide clusters could be suitable for further characterisation of the texture with reference to the mechanical properties. The use of hierarchical skeletons as described in Pirard [4] is under investigation.

Even if the grain boundaries are partially defined by carbides (Figure 10), the grain size can be measured by the intercept method [5] that yields an average intercept length inside grain phase, which is the average of intercept lengths measured every 9 degrees and on lines spaced by 4 pixels.

RESULTS

Area Fraction

Table 4 lists the results of the mean area fraction for each direction. Surface fractions of every carbide type are similar for the three directions except the M_2C fraction and consequently the total carbide fraction, which are bigger for the surface 3. An explanation will be advanced later when studying the M_2C size.

Table 4. Area fraction for the three main directions in the shell (150 images analysed per direction).

Surface	MC Area fraction	M2C area fraction	M7C3-M6C area fraction	Carbide area fraction
S1	6.0 %	1.5 %	6.8 %	14.3 %
S2	6.1 %	1.1 %	7.2 %	14.4 %
S3	6.3 %	2.7 %	7.3 %	16.2 %

Carbide size

For MC and M_2C carbides, the length of the major axis of their ellipse of inertia increases from the surface to the core. On Figure 11, for the surface 1, the average axis length of the second sample is biased. On images acquired of this analysed sample, the matrix was dirtier because the etching did not work as well as on the other samples. Boundaries of matrix around clusters are so thick that they are undeleted and considered like MC. These false MC are smaller and induce a decrease of the average axis length.

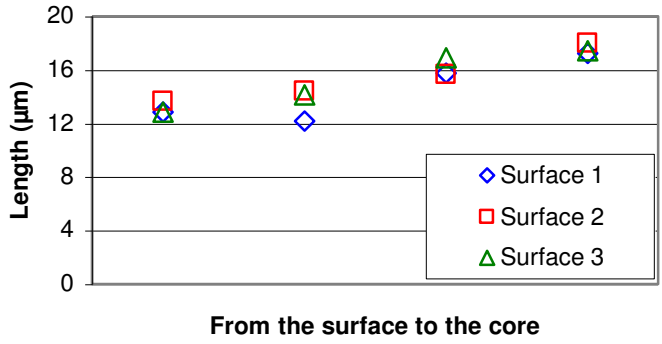

Fig. 11: Evolution of the major axis length of MC carbides along the shell depth (more than 4000 MC analysed per section).

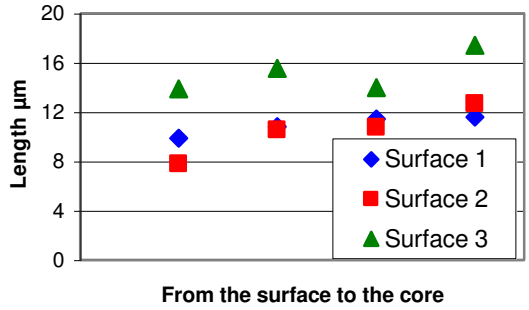

Fig. 12: Variation of the M_2C major axis length versus the depth (more than 2000 M_2C analysed per section).

The surface fraction and the average axis length of M_2C are larger on surface 3 because fibrous M_2C have a preferential orientation. Their largest dimension is orientated nearly parallel to the transverse direction of the cylinder.

Grain Size

Figure 13 presents the average intercept length in grains versus the depth. The increasing trend of this parameter confirms the grain size increase visually observed.

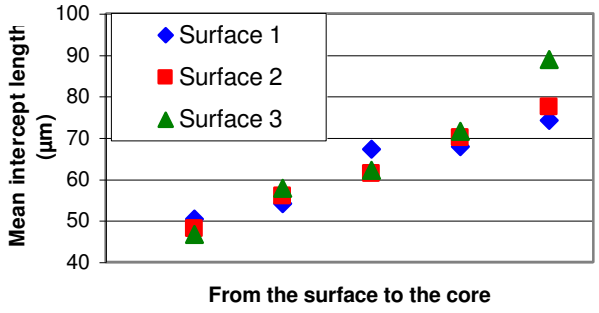

Fig. 13: Average intercept length from the roll surface to the core.

DISCUSSION

Because size variations are important along the shell depth, images cannot be acquired with a single magnification. With a large magnification (distance between two pixels 0.44 µm), some parameters (like the cluster skeleton length) reach a sill near the core because all large

particles not totally included in an image are not measured. With a two times smaller magnification (distance between two pixels 0.88 µm), resolution is too weak to characterise the smallest carbides. So, a magnification change is necessary from the surface to the core.

Because surface fractions are no additive if the areas of analysed images are different, the future acquisition process would be the next one:

- For samples near to the surface, images acquired with a 20 times magnification and a resolution of 1280 by1024 squared pixels.
- For samples near to the core, images acquired with a 10 times magnification and a resolution of 640 by 512 squared pixels.

In that way, the area fraction will be always measured on the same surface (0.063 mm² per image) and the covered field will be able to characterise even the largest clusters.

Etching result influences the carbide quantification. So, for a better carbide segmentation, the Groesbeck's etching should be much more reproducible. Image processing should be also reviewed to delete functions with parameters very sensible to a dirty matrix or to colour variations.

CONCLUSIONS

Parameters describing carbide and grain size present the trend suspected by qualitative observations: an increase of their size from the surface to the core. This observation can be correlated to the industrial process: the solidification is faster near the surface of the roll, leading to smaller carbides and smaller grain size. Other parameters must be defined to quantify the M_6C-M_7C_3 and cluster size. Some algorithms will be also written to quantify the fraction of intercellular MC carbides, which have been shown to improve the fracture behaviour [8].

ACKNOWLEDGEMENTS

The authors thank the society Marichal-Ketin S.A. for the materials and helpful information.

REFERENCES

[1] VANDER VOORT G.F., Metallography and microstructures. ASM Handbook, Vol 9, p 257.
[2] COSTER & CHERMANT, 1985. Précis d'analyse d'images, CNRS Ed. Paris.
[3] MEDALIA A.I., 1970. Dynamic shape factors of particles. Powder Technol., 4: 117-138.
[4] PIRARD E., LEBRUN V., NIVART J.-F. July 1999. Optimal acquisition of video images in reflected light microscopy. Microscopy and Analysis, 9-11.
[5] LAUNEAU P., 1996. Fabric analysis using the intercept method, Tectonophysics 267, 91-119
[6] RUSS J.C., 1999. The image processing. Handbook. CRC Press.
[7] PIRARD E. 1996. The Holodisc distance transform and its application in image analysis. Microsc. Microanal. Microstrut. 7. 453-460.
[8] HWANG K.C., LEE S., LEE H.C., 1998. Effects of alloying elements on microstructure and fracture properties of cast high-speed steel rolls. Materials Science and Engineering, A254 282-304.